

Utah State University

DigitalCommons@USU

---

International Junior Researcher and Engineer  
Workshop on Hydraulic Structures

7th International Junior Researcher and  
Engineer Workshop on Hydraulic Structures  
(IJREWHS 2019)

Jun 25th, 12:00 AM - Jun 27th, 12:00 AM

## Modeling of a Novel Submerged Oscillating Water Column (SOWC) Energy Harvester

Mohammadamin Torabi

Idaho State University, [toramoha@isu.edu](mailto:toramoha@isu.edu)

Bruce Savage

Idaho State University, [savabruc@isu.edu](mailto:savabruc@isu.edu)

Follow this and additional works at: <https://digitalcommons.usu.edu/ewhs>

 Part of the [Civil and Environmental Engineering Commons](#)

---

Torabi, Mohammadamin and Savage, Bruce, "Modeling of a Novel Submerged Oscillating Water Column (SOWC) Energy Harvester" (2019). *International Junior Researcher and Engineer Workshop on Hydraulic Structures*. 8.

<https://digitalcommons.usu.edu/ewhs/2019/Session1/8>

This Event is brought to you for free and open access by the Conferences and Events at DigitalCommons@USU. It has been accepted for inclusion in International Junior Researcher and Engineer Workshop on Hydraulic Structures by an authorized administrator of DigitalCommons@USU. For more information, please contact [digitalcommons@usu.edu](mailto:digitalcommons@usu.edu).



## **Modeling of a Novel Submerged Oscillating Water Column (SOWC) Energy Harvester**

Mohammadamin TORABI

Ph.D. candidate, Department of Civil and Environmental Engineering, Idaho State University, USA,  
toramoha@isu.edu

Bruce SAVAGE

Associate Professor, Department of Civil and Environmental Engineering, Idaho State University,  
USA, savabruc@isu.edu

**Abstract:** Wave energy converters (WEC) are hydraulic structures that are used to harvest energy from oceans. This research explores a new concept of a WEC termed a Submerged Oscillating Water Column (SOWC). Numerical simulations using the Computational Fluid Dynamics (CFD) code Flow-3D and physical model tests were carried out at Idaho State University to assess the validity and efficiency of the proposed device. The SOWC device consists of two submerged chambers that are connected to allow airflow between the two as waves pass; ideally spaced at half a wavelength. The results of the CFD modeling for seventeen different geometries with linear waves were investigated. The model was validated with experimental tests in a flume and the efficiency of the device calculated. The influence of four parameters: water depth, wave height, period and the size of SOWC were investigated. The numerical CFD modeling indicates the ratio of water elevation movement inside the chambers can be up to 80% of wave height. The numerical and physical models indicate that the concept of the SOWC works.

**Keywords:** Submerged oscillating water column(SOWC), wave tank, wave energy

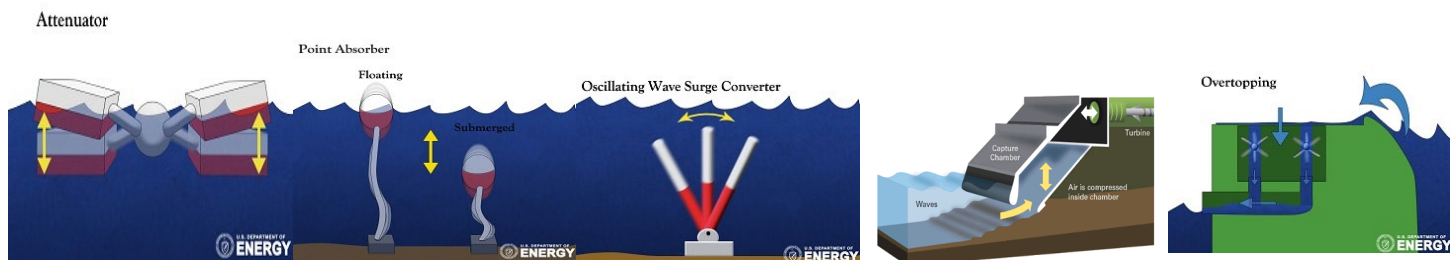
### **INTRODUCTION**

Due to potential shortages of fossil energy, many countries are interested in using renewable energy. Suitable renewable energy alternatives are required to maintain and even improve our standard of living. As more than 40% of the US population lives within 50 miles of a coastline, wave energy has the potential to provide a local renewable natural resource to a large share of the US population. There exists a significant amount of energy within waves that can be extracted (Jacobson et al. 2011).

Typical ocean waves are generated by wind interacting with the ocean surface. These wind-blown waves can travel large distances over deeper parts of oceans without a significant loss of energy. However, wave velocities slow down in nearshore regions due to bed friction and bottom

slope. This causes the wavelength to decrease and the height to increase that leads to breaking waves at certain locations when the ratio of wave height to wavelength is 1 to 7 (Cruz 2007). The total wave energy resource along the outer continental shelf estimated by EPRI is 2,640 TWh/yr (Washington, 2019). Considering that 1 TWh/yr can supply the power for approximately 93,850 U.S. homes annually (Jacobson et al. 2011), there is a significant potential for wave energy. Different Wave Energy Converters (WEC) have been invented to capture ocean wave energy in the last century. These devices are categorized by the installation location as shoreline, nearshore and offshore or the Power Take-Off (PTO) system. Also, most devices can be characterized as belonging to one of six types: Attenuator; Point Absorber; Oscillating Wave Surge Converter (OWSC); Oscillating Water Column (OWC); Overtopping Device and Submerged Pressure Differential (Figure 1). Alamian et al. 2014 outlines attenuators such as the Pelamis and the Anaconda. Point Absorbers are single floats on the surface absorbing energy from all directions generating 250 kW to 1MW. These include Columbia Power(CPT) (Rhinefrank et al. 2010; Brekken 2010), OPT- PB 500 (Dufera 2016), Finavera (Callaway 2007), Seabased/ Uppsala Univ., Archimedes Wave Swing, SeaRev (Ruellan et al. 2010) and Wavebob (Weber et al. 2009). OWSCs extract energy through an oscillating arm and OWCs are partially submerged devices that are open to the sea below the water surface and with a column of air that raises and lowers with the waves such as Wavegen and Oceanlinx with 500kw and 1.5 MW generated power respectively (Drew et al. 2009). Submerged pressure differential devices are typically located nearshore and attached to the seabed. The motion of the waves causes the sea level above the device to increase and decrease which leads to a pressure differential in the device. Archimedes Wave Swing is an example of this device (Valério et al. 2007). The proposed device has the benefit of minimizing the environmental and aesthetical impacts, ability to weather severe weather events. Also, it can develop a low cost, high-performance solution.

Figure 1: wave energy devices; left to right: Attenuator, point absorber, OWSC, OWC, Overtopping (Wave, 2019)

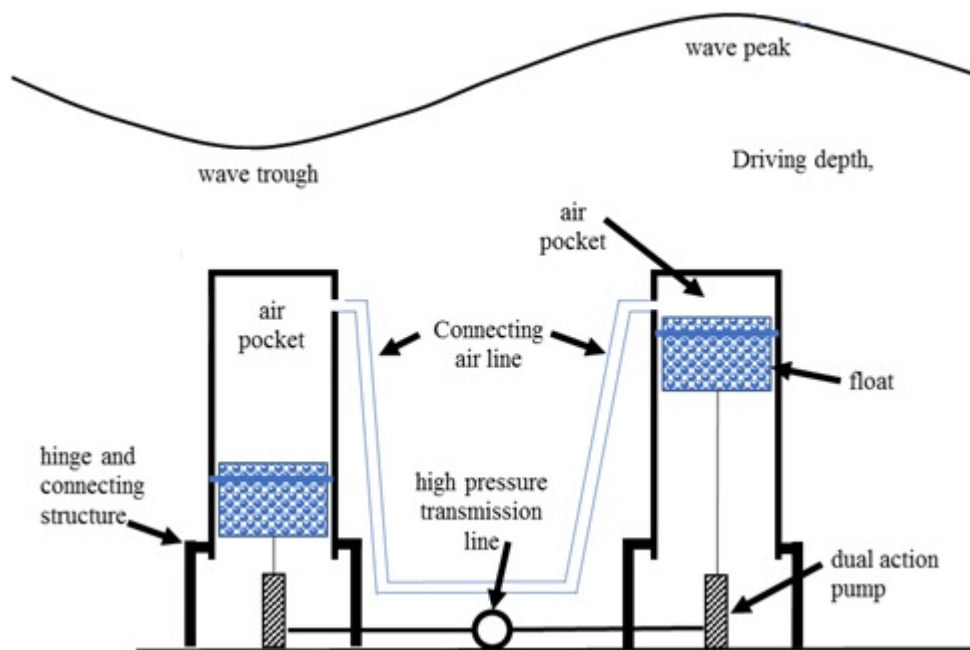


## CONCEPTUAL SOWC

This study explores a novel submerged oscillating water column (SOWC), that combines the existing technology of point absorbers, and oscillating columns. The proposed SOWC is constructed by inverting a pipe, capping one end and embedding a float/buoy inside the cylinders connected in series as shown in Figure 2. The vertical pipe is attached to the seafloor and an air pocket is maintained at the top of the pipe creating an air/water surface for a float. This structure by itself would be useless. However, by linking the air reservoirs of multiple SOWCs, it allows a constant pressure to be maintained between the SOWCs. The pressure within the SOWC is similar to the wave surface with a constant pressure.

As waves move across the ocean surface, peaks and troughs create oscillating hydrostatic pressure differentials on the ocean floor. By placing SOWCs one-half of a wavelength apart, one SOWC experiences an increase in pressure, while the other SOWC sees a decrease in pressure. Connecting the air reservoir between the two SOWCs allows the air to move between the devices, with the increased pressure raising the water surface inside one column while the decreasing pressure lowers the water surface in the other column. As noted previously, a float inside the SOWC will use the principle of buoyancy to drive a shaft connected to a pump, converting wave energy to mechanical energy. Computational Fluid Dynamics (CFD) and a small-scale physical model in a one-foot flume were used for proof of concept. For the numerical model, a solid model was constructed using CAD and exported to a commercially available CFD code, Flow-3D®.

Figure 2. Linked Submerged Oscillating Water Column Concept



## NUMERICAL MODELING

The numerical method in this study was based on solving the Reynolds-averaged Navier–Stokes (RANS) equations with a finite-volume method. CFD can solve and analyze fluid flow problems based on the Navier-Stokes equations. Continuity and momentum, equations (1) and (2), respectively, govern the motion of the fluid.

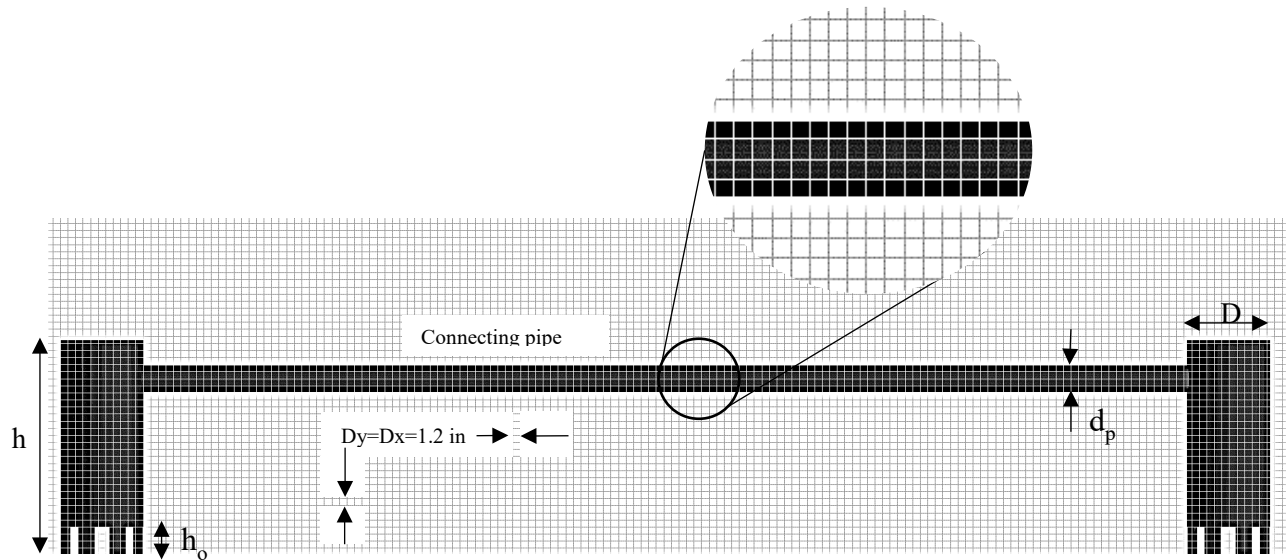
$$\frac{\partial}{\partial x}(uA_x) + \frac{\partial}{\partial y}(vA_y) + \frac{\partial}{\partial z}(wA_z) = 0 \quad (1)$$

$$\frac{\partial U_i}{\partial t} + \frac{1}{V_F} \left( U_j A_j \frac{\partial U_i}{\partial x_j} \right) = -\frac{1}{\rho} \frac{\partial P'}{\partial x_i} + g_i + f_i \quad (2)$$

The variables  $u$ ,  $v$  and  $w$  are velocities in the  $x$ ,  $y$ , and  $z$  directions;  $V_F$  is the fluid volume fraction in each cell and can be empty, full, or partially filled with fluid that gives the value of zero, one or between zero and one.  $A_x$ ,  $A_y$ , and  $A_z$  shows the fraction of open level in  $x$ ,  $y$ , and  $z$  directions;  $\rho$  is the density;  $P'$  is the pressure, and  $g_i$  is the gravitational force. The variable  $f_i$  represents the Reynolds stresses (Savage and Johnson, 2001). Turbulence was modeled using the Renormalized Group (RNG) Theory. Since a volume of air is contained in the top region of the SOWSs, the air was modeled as a void region using an adiabatic bubble with an assigned void pressure rather than model it as a second fluid. In essence, Flow-3D treats the airflow as a confined adiabatic bubble. The bubble model evaluates the void region pressure based on the volume by using the isentropic model of expansion/compression in which  $PV^\gamma$  is constant.

The grid domain consisted of three linked and one embedded mesh blocks (Figure 3) with over 487,500 total cells. The motion of the floating buoys was modeled as a moving solid. The geometry was constructed from baffles and solids. The total flow domain was greater than four times the wavelength ( $4\lambda$ ). Boundary conditions included sidewalls ( $y$ -direction) with symmetry boundaries; top boundary ( $z$ -max) as a pressure boundary with atmospheric pressure equal to 2116 lbf/ft<sup>2</sup>; bottom boundary as a wall; left upstream inlet side ( $x$ -min) as a wave boundary; and the downstream ( $x$ -max) as an outflow with a non-moving wave absorbing layer (sponge layer) to prevent wave reflections back into the model. Figure 3 shows the solid model imported into the constructed numerical grid. The pipe between the two SOWC cylinders allows air motion as waves pass. The ideal distance between chambers is considered a half of a wavelength, placing the peak of one wave above one cylinder while the trough is simultaneously over the second cylinder. Seventeen different numerical simulations were completed by varying the cylinder height,  $h$  (two and three feet); water depth,  $d$  (four- eight ft); cylinder diameter,  $D$  (constant at 1 foot); wave period,  $T$  (1.75 s- 3.0 s); and wavelength,  $L$ . Configurations are shown in Table 1 with the results.

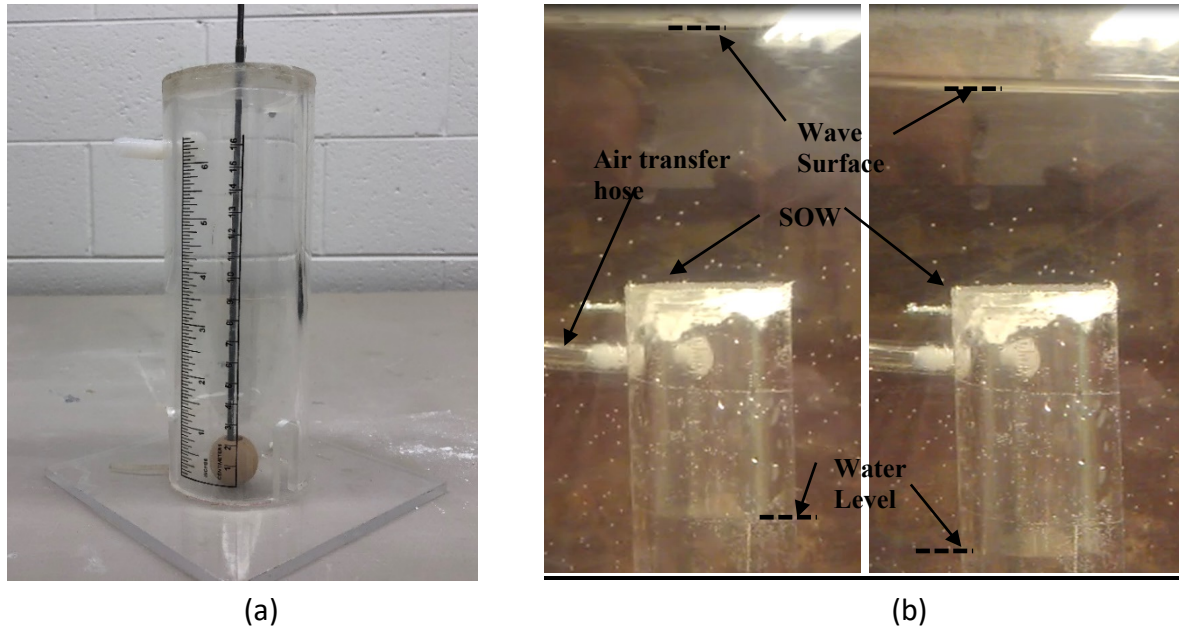
Figure 3: SOWC meshing



## EXPERIMENTAL TESTS

In order to verify the numerical data, a simple physical model was also constructed. The experiments were completed in a one ft wide x 16ft long flume with a maximum depth of one foot. A sinusoidal wave generator is capable of making regular waves with different lengths and heights. To measure the oscillating water surface inside the chambers, a long thin rod was placed in a hole drill in the top of a closed three-inch diameter transparent pipe. A wood buoy was placed inside the cylinder to track the water motion inside as shown (Figure 4a). Two of the cylinders were placed approximately a half of the average wavelength apart and connected by a flexible three-eighth inch hose. The initial air pocket was placed in the SOWC using the flexible hose. The hose allowed air to travel between the SOWCs as the waves moved over the cylinders. Unfortunately, instrumentation for the flume/waves was limited and the results from this study were more qualitative than quantitative. Figure 4b shows one SOWC with the changing water surfaces.

Figure 4: (a) Single SOWC model; (b) water level inside the SOWC columns with waves.



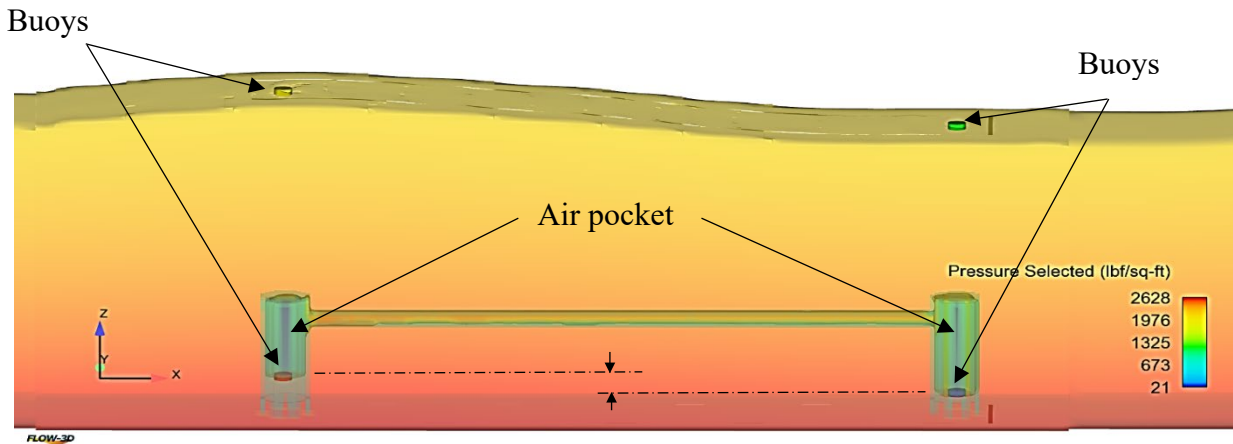
## METHOD AND MATERIAL

In this study, Flow-3D was used for the numerical modeling. The dual 3.4 GHz quad-core computer had 64 GB RAM and took 6 to 24 hrs to complete 30s of simulated flow time. Floating buoys were placed inside and directly above each SOWC to track the water surface movement (Figure 5). The buoys were constrained to only move in the z-direction. After reaching quasi-steady state, the buoys' motion over time was exported and plotted (Figure 6). The difference between adjacent peaks and troughs were calculated and averaged and the efficiency is measured by dividing the relative movement of subsea buoys to floated buoys and defined as:

$$\varepsilon = \frac{a_c}{a_i}$$

where  $a_c$  is the amplitude of water surface inside the cylinders and  $a_i$  is the amplitude of incident waves. The dimensionless relative depth parameter  $\frac{d}{gT^2}$  was calculated to find the relation with efficiency.

Figure 5: Simulated SOWC device



## RESULTS AND DISCUSSION

The CFD modeling provided realistic results for the SOWC simulations. By increasing the relative movement of the water surface inside the cylinders to wave height, the efficiency of the device increases. Table 1 indicates generated wave parameters, dimensionless relative depth, and average efficiency of left and right subsea buoys and total average. The diameter of the cylinders was 1 ft and the height was 2 or 3 ft; mentioned in the table 1. Test No#6 in Table 1 has the highest efficiency of 82% and test no#11 has the lowest of 30%. The reason is the relative depth; by increasing the depth the efficiency would decrease which is observable in *Figure 7*. The graph in *Figure 7* indicates the relative depth and total average efficiency of the buoys. It shows a correlation of  $R^2=0.96$  between relative depth and efficiency in the intermediate water depth. According to the definition,  $0.05 < d/L < 0.5$  is a intermediate water depth (Sorensen, 2005). The results of Table 1 indicate that the SOWC device is in an intermediate water depth.

Figure 6: Analysis of buoy motion to water surface motion



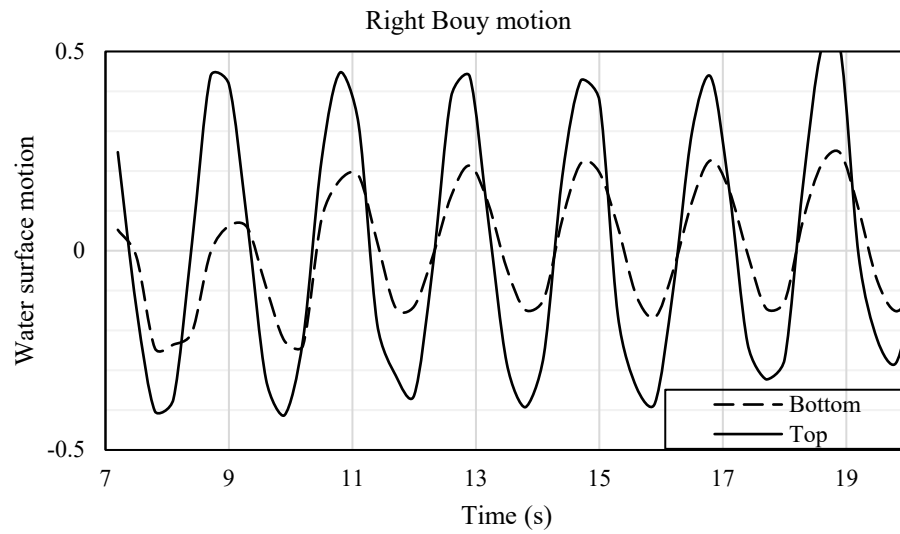
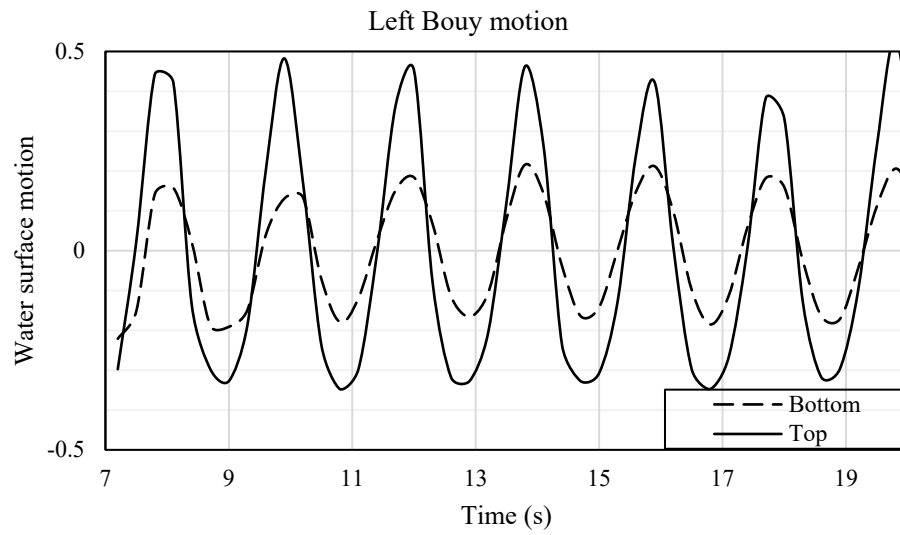
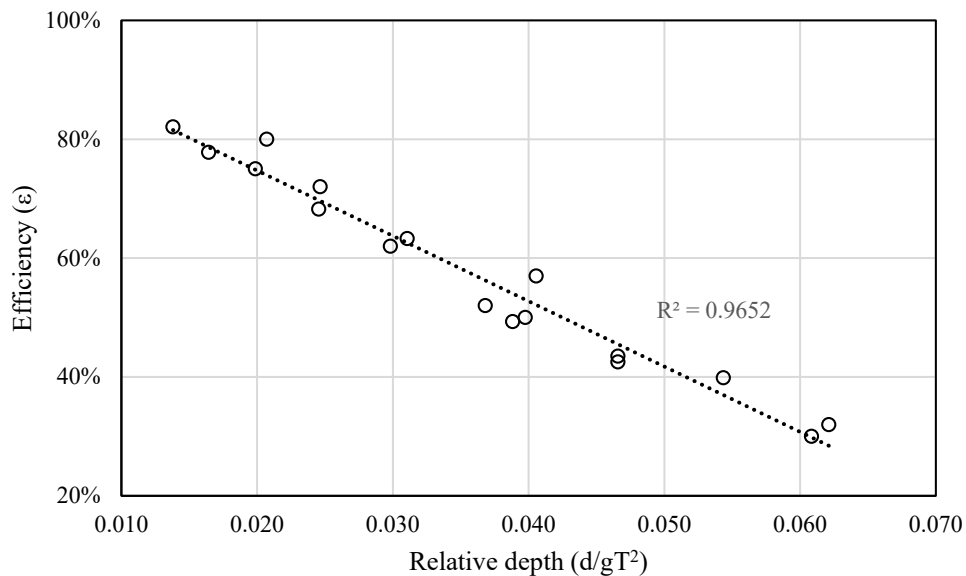


Table 1: Numerical result analysis of the tests

Test No	h	d	T	L (ft)	d/L	d/gT <sup>2</sup>	Left Buoy	Right Buoy	ave
1	2	4	1.75	14.69	0.272	0.041	55.3%	58.6%	57.0%
2	2	4	2.00	18.09	0.221	0.031	61.4%	65.2%	63.3%
3	2	4	2.25	21.41	0.187	0.025	65.9%	70.7%	68.3%
4	2	4	2.50	24.64	0.162	0.020	74.6%	75.5%	75.0%
5	2	4	2.75	27.81	0.144	0.016	80.0%	75.6%	77.8%
6	2	4	3.00	30.93	0.129	0.014	85.1%	79.0%	82.1%
7	2	5	2.00	19.03	0.263	0.039	47.6%	51.0%	49.3%
8	2	6	2.00	19.63	0.306	0.047	42.6%	42.5%	42.5%

9	2	7	2.00	19.99	0.350	0.054	39.6%	40.2%	39.9%
10	2	8	2.00	20.21	0.396	0.062	32.8%	31.1%	32.0%
11	3	6	1.75	15.45	0.388	0.061	29.8%	30.2%	30.0%
12	3	6	2.00	19.63	0.306	0.047	41.0%	46.0%	43.5%
13	3	6	2.25	23.83	0.252	0.037	50.6%	53.4%	52.0%
14	3	6	2.50	27.96	0.215	0.030	63.0%	61.0%	62.0%
15	3	6	2.75	32.02	0.187	0.025	70.0%	74.0%	72.0%
16	3	6	3.00	35.99	0.167	0.021	78.0%	82%	80.0%
17	3	8	2.50	29.87	0.268	0.040	52.0%	48.0%	50.0%

Figure 7: Relative depth to efficiency graph



## CONCLUSION

In this research, a new conceptual submerged device for capturing the ocean wave energy is proposed. The device consists of two cylinders placed half a wavelength apart to be more efficient. Numerical and experimental results indicated the validity of surface waves generating oscillating motion in SOWCs. Analyzing the numerical results showed that the interior motion can reach up to 80% of the surface motion. Also, the difference of efficiency in this submerged SOWC, is compensable by syncing several SOWC devices and connecting them together. The results show the efficiency in intermediate water depth has a good agreement with relative depth. By increasing the relative depth the efficiency decrease. Based on the analysis, the most efficient location for the device to have higher efficiency is when the relative depth is low and waves height are big, which means the location before waves break ( $H/L \geq 1/7$ ).

Suggested future research would be the experimental tests of more than two SOWCs syncing together and compare the experimental and numerical results. With more than two SOWCs connected, the overall system efficiency, including pumps should be studied.

## NOTATION

$A_x$	fraction of open level in x directions
$A_y$	fraction of open level in y directions
$A_z$	fraction of open level in z directions
$a_c$	amplitude of water surface inside the cylinders
$a_i$	amplitude of incident waves
$d$	Water depth
$f_i$	Reynolds stresses
$g$	gravity
$h$	Height of the cylinder
$L$	Wave length
$P'$	pressure
$T$	Wave period
$V_F$	fluid volume fraction
$u$	velocities in x direction
$v$	velocities in y direction
$w$	velocities in Z direction
$\rho$	density

## REFERENCES

- Alamian, R., Shafaghat, R., Miri, S. J., Yazdanshenas, N., & Shakeri, M. (2014). Evaluation of technologies for harvesting wave energy in Caspian Sea. *Renewable and Sustainable Energy Reviews*, 32, 468-476.
- Brekken, T. (2010). Fundamentals of ocean wave energy conversion, modeling, and control. In *2010 IEEE International Symposium on Industrial Electronics* (pp. 3921-3966). IEEE.
- Callaway, E. (2007). Energy: to catch a wave. *Nature News*, 450(7167), 156-159.
- Cruz, J. (2007). *Ocean wave energy: current status and future perspectives*. Springer Science & Business Media.
- Drew, B., Plummer, A. R., & Sahinkaya, M. N. (2009). A review of wave energy converter technology. *Proceedings of the Institution of Mechanical Engineers, Part A: Journal of Power and Energy*, 223(8), 887-902. <https://doi.org/10.1243/09576509JPE782>
- Dufera, H. (2016). *PB500, 500 KW Utility-Scale Powerbuoy Project* (No. DOE-OPT-EE0003645). Ocean Power Technologies Inc., Pennington, NJ (United States).
- Rhinefrank, K., Schacher, A., Prudell, J., Cruz, J., Jorge, N., Stillinger, C., ... & Yim, S. (2010). Numerical and experimental analysis of a novel wave energy converter. In *ASME 2010 29th International Conference on Ocean, Offshore and Arctic Engineering* (pp. 559-567). American Society of Mechanical Engineers.
- Ruellan, M., BenAhmed, H., Multon, B., Josset, C., Babarit, A., & Clement, A. (2010). Design methodology for a SEAREV wave energy converter. *IEEE Transactions on Energy Conversion*, 25(3), 760-767.
- Sorensen, R. M. (2005). *Basic coastal engineering* (Vol. 10). Springer Science & Business Media.

- Valério, D., Beirão, P., & da Costa, J. S. (2007). Optimization of wave energy extraction with the Archimedes Wave Swing. *Ocean Engineering*, 34(17-18), 2330-2344.
- Washington, F. (2019). WAVE ENERGY CONVERSION. *The Military Engineer*.
- Wave, (2019, September 1). Capturing energy from waves with a point absorber buoy, surface attenuator, oscillating water column, or overtopping device. Retrieved from <https://tethys.pnnl.gov/technology-type/wave>.
- Weber, J., Mouwen, F., Parish, A., & Robertson, D. (2009). Wavebob—research & development network and tools in the context of systems engineering. In *Proc. Eighth European Wave and Tidal Energy Conference, Uppsala, Sweden* (pp. 416-420).